

CHEMICAL FUNDAMENTALS OF COAL CHAR  
FORMATION

S. E. Stein, R. L. Brown, L. L. Griffith, and M. Manka

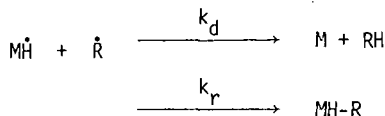
Chemical Kinetics Division, The National Bureau of Standards  
Washington, DC 20234

Recent results and current directions of our program aimed at elucidating fundamental chemical features of carbonization processes will be discussed. This program is divided into three related components: (1) elementary rate constant determinations; (2) mechanistic studies of polyaromatic pyrolysis and; (3) theoretical studies of very large, highly-condensed polyaromatic molecules. Each of these areas are discussed below.

(1) Elementary Rate Constant Determination

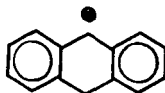
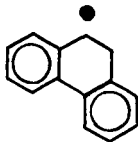
Analyses of complex reaction mechanisms generally require numerous rate constant estimates. While rate constants for many reactions of concern in thermal aromatic chemistry may be estimated with reasonable accuracy [1], several serious problem areas exist. Our rate constant measurements are devoted to such areas.

We have completed a study of relative rates of radical-radical disproportionation and recombination,  $k_d/k_r$ , for reactions involving hydroaromatic radicals,  $M\dot{H}$ ,



These ratios were derived from product concentrations in experiments where a free-radical initiator (di-tert-butyl peroxide) was decomposed at 150°C in the presence of  $MH_2$  and RH molecules.

Results of these studies are shown in Figure 1 where they are plotted against disproportionation enthalpy,  $\Delta H_d$ . Recombination rate constants are known to be relatively independent of reaction thermochemistry. Particularly noteworthy is the finding that radicals I are much more prone to disproportionation than are radicals II



The overall correlation between  $\Delta H_d$  and  $k_p/k_d$  is only fair (correlation coefficient = 0.7), but is apparently real and might be substantially improved when more accurate bond strength data are available. Moreover, based on known activation energies for related H-atom abstraction reactions [2], it would be surprising if such a dependence did not occur at low enough exothermicities. The above correlation does not hold for reactions of non-aromatic radicals [3]; this is presumably a result of the generally higher exothermicity for these reactions.

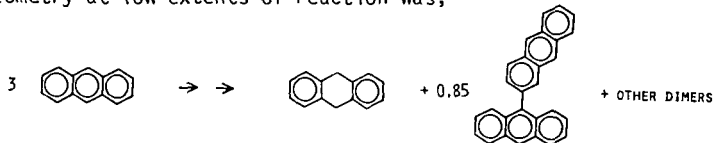
These results suggest that the highly-stabilized radicals detected in coal reactions by ESR [4] may be ineffective H-transfer agents since the only thermodynamically feasible H-transfer path open to these radicals involves disproportionation [1c].

In a series of experiments involving polyaromatic free radicals it was found that steric effects can have a profound influence on radical reactivity. For instance at 300°C H-transfer to diphenylmethyl radicals,  $\phi_2\dot{C}H$ , from the sterically-crowded molecule 1,1,2,2-tetraphenylethane,  $\phi_2CHCH\phi_2$ , occurred only 1/400 as fast as transfer from tetralin. In another series of experiments it was found that at 275°C, homolysis of 1,1,2,2-tetraphenylethane and 9,9'-bifluorene (  ) occurred > 100 times faster than predicted in the absence of strain due, presumably, to relief of steric crowding during bond breaking. Because of the large sizes of molecules and radicals involved in carbonization processes, such steric effects may be major factors controlling these reactions.

## (2) Mechanistic Studies of Polyaromatic Pyrolysis

Reaction mechanisms involved in the initial stages of carbonization are being investigated in model systems. Studies have focused on the liquid-phase pyrolysis of anthracene and phenanthrene. We have found that mechanisms of pyrolysis of these two seemingly related substances are entirely different.

In the pyrolysis of neat anthracene, An, at 350-470°C, the observed stoichiometry at low extents of reaction was,



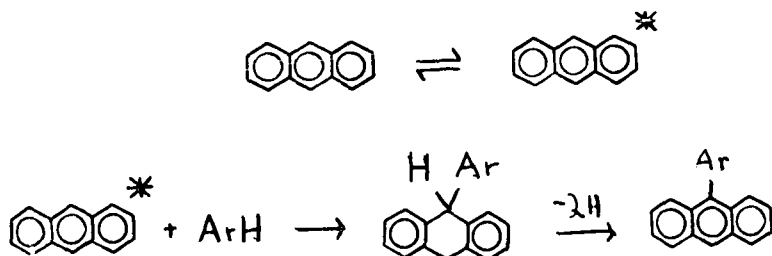
Production of anthracene dimers followed the rate expression (in moles  $l^{-1}s^{-1}$ ),

$$\frac{d[\text{dimers}]}{dt} = 10^{8.0} \exp\{-22900/T(K)\} [\text{An}]^2$$

Anthracene-solvent adducts were formed readily even in relatively inert "solvents" such as biphenyl. These adducts were generally formed with a rate constant within a factor of two of that for anthracene dimer formation.

Rates of these reactions were only slightly affected by addition of radical-forming agents such as 9,10-dihydroanthracene. In the gas phase, four dimers were formed at comparable rates and kinetics followed a more complex rate law.

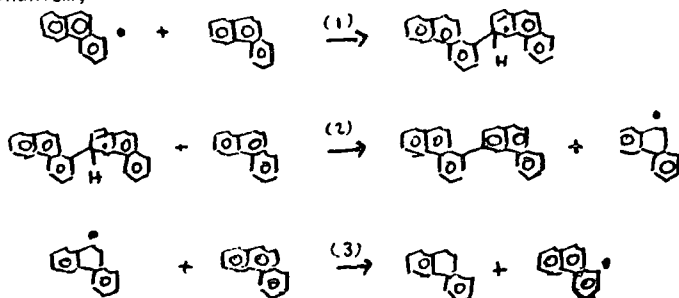
The overall kinetics for the condensed-phase reaction is consistent with the following mechanism,



where ArH may be any aromatic molecule (including anthracene itself).

Our working hypothesis is that the species is a highly reactive, charge-transfer-like intermediate. This mechanism was very unexpected on the basis of known mechanisms for gas-phase pyrolysis and differs substantially from a mechanism proposed by one of us using free-radical reaction rate arguments [5].

Phenanthrene thermolyzes much more slowly than does anthracene and displays different kinetics. At low extents of reactions in pure phenanthrene, at 400°-500°C dimers are formed according to the following (preliminary) pseudo-first-order rate expression,  $10^{8.6} \exp(-25500/T) s^{-1}$ . The rate is accelerated by free-radical generating additives (9,10-dihydrophenanthrene, for instance), the mechanism is very unselective (eight dimers of comparable amounts are formed), and gas- and condensed-phase product distributions are similar. The reaction appears to proceed via an aryl free radical-chain mechanism,



Steps 2 and 3 may involve free H-atom intermediates.

We presume that the primary factor causing the difference in mechanism between anthracene and phenanthrene is the presence of much more accessible (lower energy) "excited states" in anthracene. The triplet state energy, for instance, is 20 kcal mol<sup>-1</sup> lower for anthracene than phenanthrene.

Based on several preliminary studies of other model pyrolytic systems, the above aryl chain mechanism seems to be rather typical. It may also explain the gas-phase anthracene results. However, mechanisms more closely related to the one proposed for anthracene may become increasingly important as reacting molecules grow in size during carbonization and more accessible "excited states" become available.

### (3) Theory of Very Large Aromatic Molecules

In order to analyze reactions occurring in the late stages of carbonization, it is necessary to deal with very large, highly aromatic molecules. Since these molecules are too large to study experimentally, we are developing a theoretical approach intended to allow extrapolation of known reactivity properties of small molecules to these large structures.

In order to treat very large molecules, we are forced to use very simple theories [6]. Using a HP-1000 computer, we have examined molecules containing as many as 3300 carbon atoms. The theories used are Herndon's structure-resonance theory (SRT) [7] and Hückel Molecular Orbital Theory (HMO) [8]. Despite their simplicity, these theories are generally regarded as good predictors of chemical properties for benzenoid polyaromatic molecules, the type of primary concern in carbonization.

Our present work focuses on properties of hexagonally-symmetric molecules containing a single edge type. Initial members of two of these series are given in Figure 2. Thermodynamic stabilities of four series were determined by SRT and results are shown in Figure 3.

Reactivity indices derived from perturbational HMO theory [8] are illustrated in Figure 4 for a member of the most stable and least stable series. The area of each circle in this figure represents the energy required to fix a  $\pi$ -electron at the carbon atom represented by the circle. These energies are generally considered to be proportional to activation energies for reaction [8].

Hückel MO theory is used to obtain electronic energy levels. The upper third of the occupied energy levels for series A and B are shown in Figure 5. These levels, particularly the highest one for each molecule, contain the electrons that are involved in chemical reactions.

These calculations establish a logical framework which may be used to examine reactions at edges of very large polyaromatic molecules. We are currently applying more accurate theories and introducing other chemical features (strain energy, for instance) with the ultimate aim of deducing chemical reaction mechanisms.

Support for this research by the Gas Research Institute, Chicago, Illinois, is gratefully acknowledged.

- 1a. Benson, S. W., "Thermochemical Kinetics" Wiley and Sons, N.Y., 1976.
- b. Stein, S. E., in "New Approaches in Coal Chemistry", ACS Symp. Ser. 69, Blaustein, et al., eds., Pittsburgh, PA, 1981, pp 97-130.
- c. Stein, S. E. in "Chemistry of Coal Conversion", Schlosberg, R. D., Pergamon Press, NY, 1984 (in press).
2. Kerr, J. A.; Moss, S. J., "CRC Handbook of Bimolecular and Termolecular Reactions", Vols. 1, 2, CRC Press Boca Raton, FL., 1981.
3. Gibian, M. J. and Corley, R. C., Chem. Rev., 73, 44 (1973).
4. Retcofsky, H. L. in "Coal Science", Vol. 1, Gorbaty et al., eds., Academic Press, 1982, pp 43-83.
5. Stein, S. E., Carbon, 19, 421 (1981).
6. Brown, R. L., J. Computational Chem. 1983 in press.
7. Herndon, W. C., Isr. J. Chem. 20, 270 (1980); J. Org. Chem. 40, 3548 (1975); *ibid* 46, 2119 (1981).
8. Heilbronner, E., Bock, H., "The HMO Theory and its Application", Interscience, N.Y., 1976.

Figure 1. Plot of Measured  $k_r/k_d$  per Transferrable H-atom vs.  $\Delta H$  for Disproportionation.  $\Delta H$  estimates were made using data discussed in reference 1c and recent data given in D. F. McMillen and D. M. Golden in Ann. Revs. Phy. Chem., Ann. Rev. Inc., Menlo Park, 1982.

Figure 2. Illustrations of First Few Members of Series A and B.

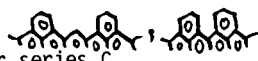
Figure 3. Log of Kekulé Structures per  $\pi$ -electron ( $KSPE \equiv n_\pi^{-1} \ln \{ \# \text{ Kekulé structures} \}$ ) Versus  $n_\pi^{-1/2}$  ( $n_\pi = \text{no. } \pi\text{-electrons}$ ). Note that  $\ln(KSPE)$  is proportional to the resonance energy per electron [7] and  $n_\pi^{1/2}$  is (nearly) proportional to the number of edge C-atoms. Series C and D have edges 

Figure 4. Electron Localization Energies for a Member of Series A(a) and B(b).

Figure 5. Upper Third of HMO Energy Levels for Series A (upper) and B(lower).

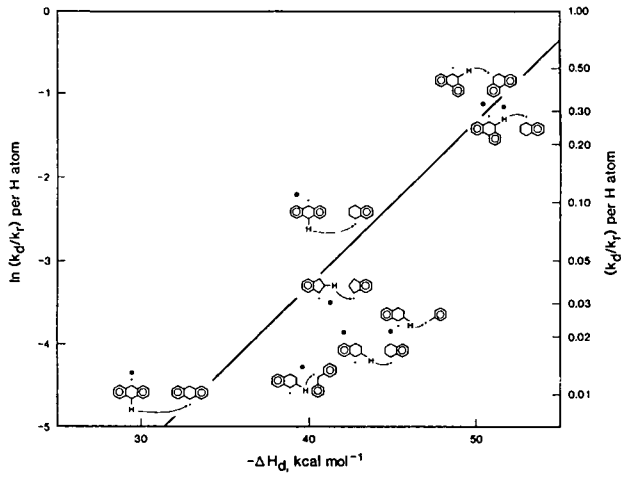


Figure 1

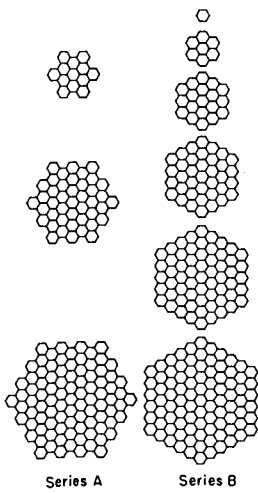


Figure 2

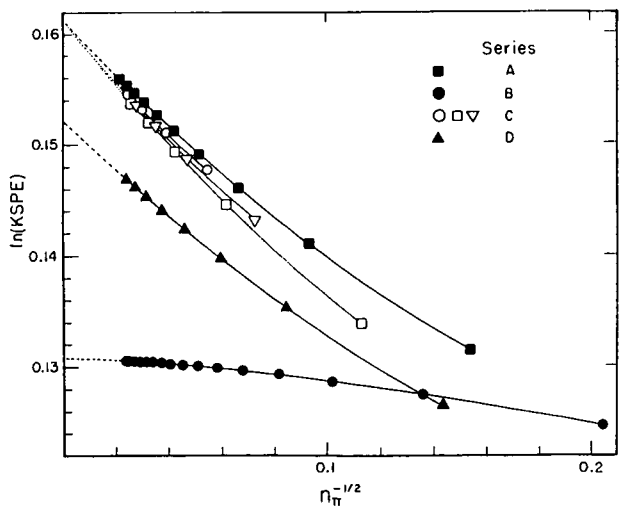


Figure 3

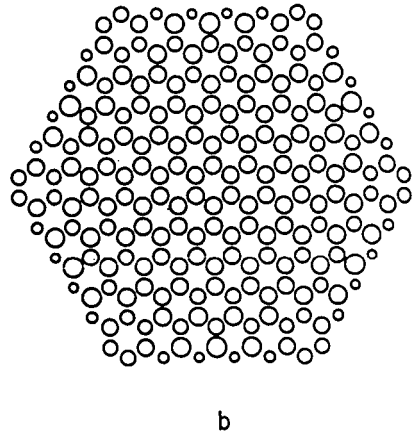
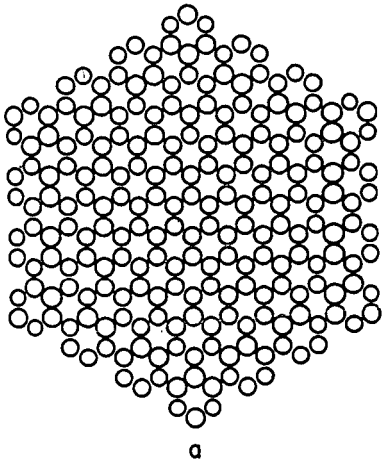


Figure 4

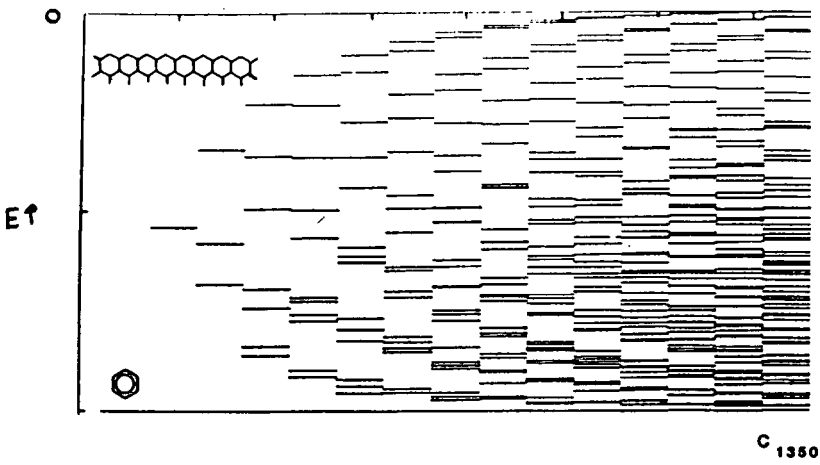
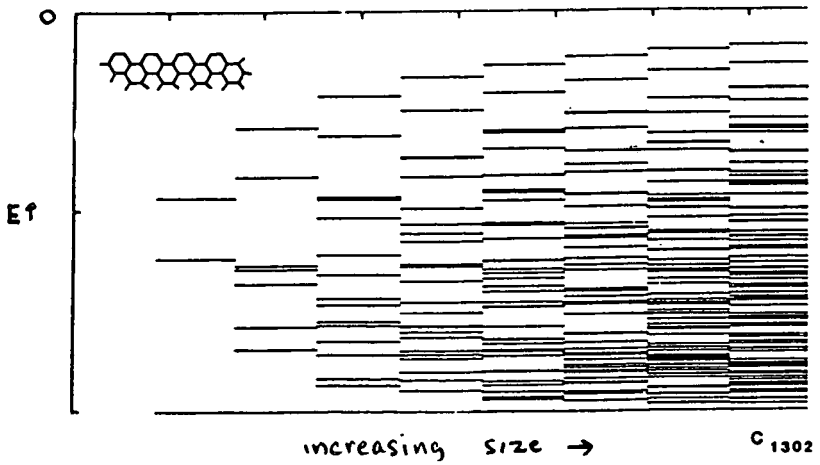


Figure 5



increasing size  $\rightarrow$